Co-published by
Institute of Fluid-Flow Machinery
Polish Academy of Sciences
Committee on Thermodynamics and Combustion
Polish Academy of Sciences

Copyright©2026 by the Authors under licence CC BY-NC-ND 4.0

http://www.imp.gda.pl/archives-of-thermodynamics/

Finding a Correlation for Predicting the Effective Thermal Conductivity of CNT Nanofluid

Farqad Rasheed Saeed[a*], Hussein Fawzi Hussein[a*], Natheer Basheer Mahmood[b]

[a]Scientific Research Commission, Baghdad, Iraq
[b]Ministry of Education, General Directorate of Baghdad Education Karkh2, Baghdad, Iraq
*Corresponding author email: hussein.f.hussein@src.edu.iq

Received: 16.06.2025; revised: 17.11.2025; accepted: 17.11.2025

Abstract

This study proposes a new correlation to predict the effective thermal conductivity of carbon-nanotube nanofluids by accounting for both carbon-nanotube characteristics (thermal conductivity, density, diameter and length) and base-fluid properties (thermal conductivity, density, specific heat, dynamic and kinematic viscosity, operating temperature and boiling point), in addition to the carbon-nanotube volume fraction. Using dimensional analysis, we constructed a set of π-groups and calibrated a regression-type model on 102 experimental data points gathered from the literature, and then assessed its accuracy against an independent set of 52 data points. Statistical indicators (mean absolute percentage error, signed mean error and standard deviation) demonstrate good agreement with measurements. Comparisons with widely used correlations further highlight the improved predictive capability of the present model, especially regarding the roles of carbon-nanotube length and diameter. Limitations: the current correlation does not explicitly incorporate nanofluid stability and aggregation metrics; thus, extrapolation beyond the calibration ranges should be made with caution. This correlation is suitable for engineering and numerical applications within the reported ranges.

Keywords: Carbon nanotubes; CNT nanofluids; Effective thermal conductivity; Dimensional analysis; Stability; Aggregation

Vol. 47(2026), No. 1, 43–53; doi: 10.24425/ather.2025.156854

Cite this manuscript as: Saeed, F.R., Hussein, H.F., & Mahmood, N.B. (2026). Finding a Correlation for Predicting the Effective Thermal Conductivity of CNT Nanofluid. *Archives of Thermodynamics*, 47(1), 43−53.

1. Introduction

Improving the thermal properties of working fluid used in different types of applications of heat transfer devices attracted the attention of researchers, which is associated with the growth of nanoparticle science [1]. The addition of nanoparticles to the base fluid to form what is known as a nanofluid enhances the thermal conductivity of the base fluid [2], and by its role improves the thermal performance of heat exchangers [3]. Nanofluids exhibit an interesting thermal behaviour that changes depending on the concentration, type, size and shape of the used nanoparticles [4]. The studies in the nanoparticles field divided into more than one competence such as, the stability of nanofluid [5,6], thermophysical properties of nanofluid [7,8], investigation of the heat transfer effects of nanofluid flow inside heat exchangers, studied both experimentally and numerically [9−12], and developing correlations to describe the effective thermophysical properties of nanofluid [13]. Most models were based on empirical data from experimental studies. Consequently, the resulting correlation is constrained by the specific experimental data and conditions used in its development and the conditions associated with the used procedure [14]. Maiga et al. [15], introduced models for predicting the effective thermal conductivity and effective viscosity of ultra-fine particles of

Nomenclature

ABS – absolute value
a – empirical constant
C – constant
d – CNT diameter, nm
k – thermal conductivity, W m^{-1} K^{-1}
l – CNT length, nm
n – shape factor
Pr – Prandtl number
T – temperature, K

Greek symbols

υ – kinematic viscosity, m^2 s^{-1}
π – dimensionless parameter
ρ – density, kg m^{-3}
Ø – volume fraction of nanoparticles, %
ψ – particle shape factor

Subscripts and Superscripts

br – Brownian motion
cal – calculated value
eff – effective property
exp – experimental value
f – base fluid
p – nanoparticle
r – reference value
ref – reference diameter

Abbreviations and Acronyms

CNT – carbon-nanotube
MAPE – mean absolute percentage error

Al_2O_3, TiO_2 and SiO_2 metal oxides based on experimental data. Simple models of Masuda et al. [16] have been used in many experimental and numerical studies. Koo and Kleinstreuer [17] used a model for predicting the effective thermal conductivity of nanofluids to study the laminar flow of nanofluids through a micro heat-sink. The model was obtained by considering experimental data of CuO nanoparticles. Das et al. [18] designed the model for thermal conductivity as a function of specific heat capacity, density of the base fluid, volume fraction of the nanoparticles, and finally, the temperature of the mixture. The range of the model validity is 0.01–0.04 volume fraction and 300–325 K in temperature. Chon et al. [19] applied the dimensional analysis to obtain a new correlation for predicting the effective thermal conductivity of Al_2O_3/water nanofluid. The correlation incorporated the following parameters: the thermal conductivity of the nanoparticles and base fluid, nanoparticle size and volume fraction, the molecular diameter of the base fluid, and the Prandtl and Reynolds numbers. The model applicability is limited for the nanoparticle size range of 11−150 nm, temperature range 294−344 K, and nanoparticles volume fraction 0.01−0.04. Prasher et al. [20] introduced a model for calculating the effective thermal conductivity of nanofluid by combining the Maxwell-Garnett conduction model with the effect of nanoparticle Brownian motion, which induces convection. The model is working with respect to the following parameters: nanoparticles volume fraction, nanoparticles size, temperature, interfacial resistance, thermal conductivity of the base fluid and thermal conductivity of the nanoparticles. The essential outcome of the model is that lighter nanoparticles improve the effective thermal conductivity of the nanofluid regardless the thermal conductivity of the nanoparticles. Sastry et al. [21] performed a theoretical model detecting the effective thermal conductivity of carbon-nanotubes (CNTs) nanofluid. The model is based on dimensionless parameters and considers the volume fraction of CNTs, shape of CNTs, their random orientation and the interaction among the CNTs. The results show an agreement of the models with experimental data. Vajjha and Das [22] investigated the effective thermal conductivity of three types of nanofluids. The used nanoparticles were Al_2O_3, CuO and ZnO. The base fluid was a mixture of ethylene glycol and water. Their experimental results had no agreement with the other models used to predict the effective thermal conductivity. They modified a model for predicting the effective thermal conductivity based on the classical model of Maxwell. The model incorporates the Brownian motion and works as a function of nanoparticles and base fluid thermal conductivity, volume fraction of the nanoparticles and temperature. The results exhibit an agreement between the model's outcomes and the experimental data.

Moghadassi et al. [23] used the dimensionless group to present a model for finding the effective thermal conductivity of Al_2O_3-water and Al_2O_3-ethylene glycol nanofluid. The model works as a function of volume fraction and particle size of alumina nanoparticles, thermal conductivity of Al_2O_3 nanoparticles, thermal conductivity of the base fluid and interfacial shell properties between the nanoparticles and base fluid. An agreement was found between the experimental data of Al_2O_3-water and Al_2O_3-ethylene glycol nanofluid and the predicted data from the model. The model also detected the effect of particle size, finding an inverse proportionality with thermal conductivity. Dimensionless groups applied by Hosseini et al. [24] were used to produce a model for predicting the effective thermal conductivity of CNTs nanofluid. The model was developed as a function of thermal conductivity of the nanoparticles, thermal conductivity of the base fluid and the effect of CNTs aspect ratio. The model shows a nonlinear behaviour with the rising volume fraction of CNTs. The comparison with the experimental data exhibits acceptable agreement. Emami et al. [25] suggested a model for estimating the effective thermal conductivity of nanofluids considering the mean distance between the particles, calculated through the Brownian motion approach. The validity of the model was achieved by comparison with the experimental data of the same work, which shows acceptable results. Patel et al. [26] performed a model to evaluate the effective thermal conductivity for metal and metal oxide nanoparticles. The model included the following parameters: nanoparticles volume fraction, nanoparticles thermal conductivity, nanoparticles diameters, temperature and base fluid thermal conductivity. The model works for the nanoparticles size ranging from 10 nm to 150 nm, nanoparticles thermal conductivity ranging from 20 W/(m·K) to 400 W/(m·K), the thermal conductivity of the base fluid ranging

from 0.1 W/(m·K) to 0.7 W/(m·K), nanoparticles volume fraction 0.001−0.03 and temperature range 293−323 K. Corcione [27] showed two empirical equations for predicting the effective thermal conductivity and effective dynamic viscosity of nanofluid. The correlation is a function of thermal conductivity of the nanoparticles and base fluid, nanoparticle volume fraction, and the Prandtl and Reynolds numbers. The model was based on collected experimental data from other studies of nanoparticles of metal and metal oxides like Cu, CuO, TiO_2 and Al_2O_3 [28−36]. The applicability of the model is in the range of nanoparticles size 10−150 nm, temperature 294−324 K and volume fraction 0.002−0.09. Azmi et al. [37] proposed a correlation for detecting the effective thermal conductivity of metal oxides nanoparticles and water-based fluid. The correlation is a function of thermal conductivity of the base fluid, thermal diffusivity of the nanoparticles, thermal diffusivity of the base fluid, temperature, nanoparticles size and nanoparticles volume fraction. The validity of the correlation is limited by the nanoparticle size 20−150 nm, temperature 293−343 K and volume fraction less than 0.04. Hosseini et al. [38] performed a nonlinear correlation for estimating the effective thermal conductivity of nanofluid. The model was generated considering the following parameters: the nanoparticle volume fraction and size, thermal conductivity of the nanoparticle and base fluid, interfacial shell properties and temperature. The model's validity was established through comparison with Al_2O_3/water experimental data, showing good agreement. All the aforementioned models are specific to particular nanoparticle types and are valid within the defined ranges of particle size, shape, temperature, volume fraction and thermal conductivity of both the nanoparticles and the base fluid.

Moreover, most models are based on and validated against experimental data from the same study or a limited number of datasets from other works. The aim of the present work is to present a model for predicting the effective thermal conductivity of CNTs using the π-terms, and based on a wide number of collected experimental data. In addition, the model covers all the parameters which may affect the effective thermal conductivity of the nanofluid. The model is also compared with experimental data from various works to detect the model's validity.

Beyond the classical thermal-conductivity models and CNT-specific correlations, several recent investigations have explored different routes for improving heat transfer in nanofluids and solar-thermal systems. Experimental and numerical analyses have demonstrated the impact of geometrical control, such as splitter-plate configurations and flow-field modifications, on the overall heat-transfer rate and stability of working fluids [65–67].

At the same time, local studies have addressed the thermal performance behaviour of solar and metallic systems under Iraqi climatic conditions, confirming the need for accurate correlations that account for temperature, viscosity and nanoparticle geometry effects [68–70]. In addition, investigations on carbon-based nanostructures such as graphene have highlighted transport similarities for CNTs, supporting the present work's emphasis on particle morphology and aggregation behaviour [71]. These recent findings collectively provide a broader context for the current correlation and validate its potential for engineering-scale thermal-modelling applications.

2. Methodology

2.1. Experimental data used to form the correlation

In order to present the correlation with acceptable accuracy, 102 data collected from different experimental investigations have been applied to derive the model. The data extracted from experimental studies have been used to characterise the thermophysical properties of CNTs/base fluid. The data contained various types of CNTs, such as multi-walled carbon nanotubes (MWCNTs) and single-walled carbon nanotubes (SWCNTs), with different lengths and diameters. Moreover, various types of base fluids were used in the mentioned experimental studies. Table 1 displays the used literature data to produce the present correlation for CNTs, and base fluids details.

Table 1. Literature data used to construct the correlation (CNT type, ranges of $\emptyset$, d, l, base fluid and T) [10].

References	Nanoparticles	$\emptyset$, %	d_p, nm	l_p, nm	Base fluid	T, K
[39]	SWCNTs	0.1	1	100−600	water	298−333
[39]	SWCNTs	0.2	1	100−600	water	298−333
[39]	SWCNTs	0.3	1	100−600	water	298−333
[40]	MWCNTs	0.04−1	25	50000	Polyalphaolefin	298
[41]	MWCNTs	0.25−1.5	50-80	10000−20000	Ethylene glycol	298
[42]	CS- SWCNTs	0.004−1.5	1−1.4	2400	Ethylene glycol	298
[42]	CNI-SWCNTs	0.004−1.1	1−1.4	1200	Polyalphaolefin	298
[43]	TCNTs	0.23−1	15	30000	Ethylene glycol	298
[43]	TCNTs	0.4−1	15	30000	Distilled water(DW)	298
[44]	MWCNTs	0.04−0.85	20−60	50000	water	293, 318
[45]	MWCNTs	0.25−1	10−30	10000−50000	water	300
[46]	CNTs	0.01−0.1	20	35000	water	298, 303
[47]	CNTs	0.1−1	10−20	10000−30000	water	293, 298, 303, 308, 313, 318

2.2. Effective thermal conductivity correlation

The effective thermal conductivity is a key parameter that governs the thermal performance of nanofluids and is influenced by other thermophysical properties, including the effective dynamic viscosity, specific heat and density. This study develops a correlation to predict the effective thermal conductivity of CNT nanofluids by incorporating all significant parameters related to both the nanoparticles and the base fluid. Using dimensional analysis [48,49], we derived the dimensionless groups (π-terms) for the correlation. Equation (1) expresses the effective thermal conductivity as a function of the following physical variables: CNT volume fraction, thermal conductivity of the base fluid and nanoparticles, Brownian velocity, specific heat capacity of the base fluid, CNT diameter and length, nanofluid temperature, boiling point of the base fluid, kinematic viscosity and a reference diameter.

Hassani et al. [50] proposed a correlation that includes most of these physical variables but omits the effect of nanoparticle length. Their model serves as a general tool for predicting the effective thermal conductivity of various nanofluids with different nanoparticles and base fluid types. However, CNTs possess a distinctive cylindrical geometry and exceptionally high intrinsic thermal conductivity, setting them apart from other nanomaterials. Therefore, the correlation presented in this work is specifically designed to predict the effective thermal conductivity of CNT-based nanofluids. The functional relationship is given by Eq. (1):

$$k_{eff} = f\left(\emptyset, k_f, k_p, v_{br}, C_{p.f}, d_p, l_p, T, d_{ref}, v_f, T_b\right). \quad (1)$$

Dimensional analysis resulted in 8 dimensionless groups, or the so-called π groups as shown in Table 2. The repetitive variables used in the derivation procedure are k_f, l_p, v_{br} and T.

Table 2. Dimensionless groups used in the correlation.

π-group	Physical variables
π_1	$\frac{k_{eff}}{k_f}$
π_2	$\emptyset$
π_3	$\frac{k_p}{k_f}$
π_4	$\frac{C_{p.f}\cdot T}{v_{br}^2}$
π_5	$\frac{d_{ref}}{l_p}$
π_6	$\frac{d_p}{l_p}$
π_7	$\frac{v_f}{l_p \cdot v_{br}}$
π_8	$\frac{T_b}{T}$
π_9	$\frac{\mu \cdot C_{p.f}}{k}$

Based on the dimensionless groups listed in Table 2 and the experimental data summarised in Table 1, the correlation was developed using a nonlinear regression analysis, resulting in Eq. (2):

$$\pi_1 = 1 + {\pi_2}^{1.02}{\pi_3}^{0.428} + 99.99{\pi_2}^{1.02}{\pi_9}^{-1.74} + -0.15{\pi_2}^{1.02}{\pi_3}^{0.428}{\pi_4}^{0.429}{\pi_5}^{0.92}{\pi_6}^{0.45}{\pi_7}^{0.56}{\pi_8}^{22.56}{\pi_9}^{-1.74}. \quad (2)$$

The Brownian motion is calculated according to Eq. (3), [51], as follows:

$$v_{br} = \sqrt{\frac{18\, k_b T}{\pi \rho_p d_p^3}}, \quad (3)$$

where d_{ref} is equal to 2.9 A° [52,53].

2.3. Correlation accuracy

The accuracy of the presented correlation Eq. (2), is measured by calculating the mean deviation, average deviation and standard deviation by using Eqs. (4), (5) and (6) [50], for the present correlation in comparison with 102 experimental data:

$$Mean\ deviation = \frac{1}{n}\sum_1^n ABS[100(\pi_{1,cal} - \pi_{1,exp})/\pi_{1,exp}], \quad (4)$$

$$Average\ deviation = \frac{1}{n}\sum_1^n [100(\pi_{1,cal} - \pi_{1,exp})/\pi_{1,exp}], \quad (5)$$

$$Standard\ deviation = \sqrt{\left(\frac{1}{n}\sum_1^n [100(\pi_{1,cal} - \pi_{1,exp})/\pi_{1,exp}]^2 - Average\ deviation^2\right)}. \quad (6)$$

2.4. Correlation validity

In order to ensure the validity of the present correlation, 52 data of external experimental studies have been used to test Eq. (2). These experimental data were not included in the database used to form Eq. (2). Table 3 shows the experimental studies used to achieve the validity of the present correlation. The results exhibit acceptable outcomes between the predicted data and the experimental data.

Table 3. Literature data used for external validation.

References	Nanoparticles	Ø, %	d_p, nm	l_p, nm	Base fluid	T, K
[54]	SWCNTs	0.03–0.2	1	150-500	Ethylene glycol	298
[55]	MWCNTs	0.006–0.3	9.2	1500	water	293
[55]	MWCNTs	0.006–0.3	9.2	1500	water	303
[55]	MWCNTs	0.006–0.3	9.2	1500	water	313
[56]	MWCNTs	0.2	11	10000	water	303–363
[56]	MWCNTs	0.5	11	10000	water	303–363
[56]	MWCNTs	0.75	11	10000	water	303–363
[56]	MWCNTs	1	11	10000	water	303–363
[57]	MWCNTs	0.3	20–30	10000–30000	water	293–318

2.5. Comparison with other models

The present correlation has been compared with previous models used to specify the effective thermal conductivity of CNTs/base fluid. The models are applied to the 154 data mentioned in Tables 1 and 3, and compared to the present correlation. One of the most used models to predict the effective thermal conductivity of nanofluid, considering the shape of nanoparticles is the Hamilton–Crosser model, Eq. (7) [58]. The model works as a function of thermal conductivity of the base fluid, nanoparticles thermal conductivity, nanoparticles volume fraction and nanoparticles shape

$$\frac{k_{eff}}{k_f} = \frac{k_p+(n-1)k_f+(n-1)(k_p-k_f)\emptyset}{k_p+(n-1)k_f-(k_p-k_f)\emptyset}, \quad (7)$$

where:

$$n = \frac{3}{\psi}, \quad (8)$$

$$\psi = \frac{surface\ area\ of\ the\ sphere}{surface\ area\ of\ the\ real\ particle\ with\ an\ equal\ volume}. \quad (9)$$

The second model used for comparison was presented by Patel et al. [59], Eq. (10), and considered a general equation for predicting the effective thermal conductivity of CNTs. The model works as a function of thermal conductivity of the base fluid, thermal conductivity of the CNTs, volume fraction of CNTs, diameter of CNTs and liquid particle size

$$\frac{k_{eff}}{k_f} = 1 + \frac{k_p \emptyset\, d_f}{k_f(1-\emptyset)d_p}. \quad (10)$$

The value of d_f was determined by Patel et al. [59] for water, so the only data for water from Tables 1 and 3 are included in the comparison.

Dimensionless groups were used by Hosseini et al. [24] in their model as given by Eq. (11):

$$\frac{k_{eff}}{k_f} = 1 + 51.84\left(\frac{1}{d}\right)^{0.441}(a_r)^{0.14}(\emptyset)^{0.749}, \quad (11)$$

where a_r is the aspect ratio, which is l_p/d_p. The model has been compared with the present correlation for 154 data items.

The last correlation used for comparison is introduced by Hassani et al. [50], Eq. (12), the correlation based on dimensionless groups and used to predict the effective thermal conductivity for all types of nanoparticles, including CNTs, as a function of all parameters which may affect the nanofluid properties, excluding the nanoparticles length

$$\frac{k_{eff}}{k_f} = 1.04 + \emptyset^{1.11}\left(\frac{k_p}{k_f}\right)^{0.33}\mathrm{Pr}^{-1.7} \times \quad (12)$$

$$\times\left[\frac{1}{\mathrm{Pr}^{-1.7}} - \frac{262}{\left(\frac{k_p}{k_f}\right)^{0.33}} + 135\left(\frac{d_{ref}}{d_p}\right)^{0.23}\left(\frac{v_f}{d_p v_{br}}\right)^{0.82}\left(\frac{C_p}{T^{-1}v_{br}^2}\right)^{-0.1}\left(\frac{T_b}{T}\right)^{-7}\right].$$

Another comparison has been made with the models of Wen and Ding [44], and Jiang et al. [56]. Experimental data were used to predict the effective thermal conductivity of the nanofluid using the present model (Eq. (2)) and four previously published models (Eqs. (7), (10), (11) and (12)).

3. Results and discussion

The present correlation, Eq. (2), was generated by applying a nonlinear regression analysis for the data mentioned in Table 1, which includes 102 data collected from different experimental studies. The correlation was verified through statistical calculations using Eqs. (4–6) to determine the mean, average and standard deviations; the results are shown in Table 4. The standard deviation was equal to 8.46%, 18.04% and 21.84% for water, polyalphaolefin and ethylene glycol, respectively. The lowest values for the mean, average and standard deviation were found for the water data, which can be interpreted by the fact that a large number of data points (78) for water were used to produce the correlation. The comparison between the experimental data from Table 1, and the predicted data by the present correlation is shown in Fig. 1.

Table 4. The comparison of the predicted data found from the present correlation with the experimental data from Table 1.

	Base fluid	Mean deviation (%)	Average deviation (%)	Standard deviation (%)	Number of data
Based on Table 1	Water	5.96	−3.08	8.46	78
	Polyalphaolefin	12.62	−10.01	18.04	11
	Ethylene glycol	19.61	19.61	21.84	13
	All data	8.42	−0.94	12.47	102

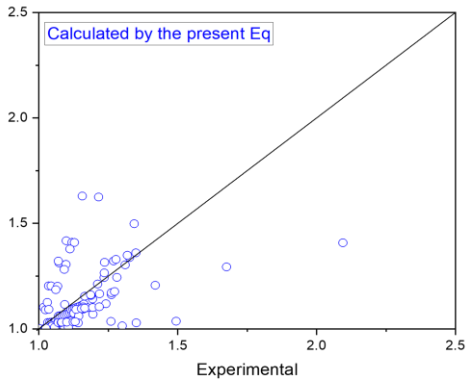

Fig. 1. The calculated data found from Eq. (2) in comparison with the experimental data from Table 1.

The validity of the correlation has been checked by testing Eq. (2) on 52 new experimental data, which were not included in the base data used to generate the correlation. The data used to validate the correlation are shown in Table 3. The validity results are shown in Table 5.

Table 5. The comparison of the predicted data found from the present correlation with the experimental data from Table 3.

	Base fluid	Mean deviation (%)	Average deviation (%)	Standard deviation (%)	Number of data
Based on Table 3	Water	12.89	4.80	15.48	46
	Ethylene glycol	2.65	−2.63	3.25	6
	All data	11.71	3.94	14.61	52

However, data for polyalphaolefin are limited; therefore, the validation was performed using only water and ethylene glycol data. The standard deviations for water and ethylene glycol were recorded at 15.48% and 3.25%, respectively, and the total standard deviation for the 52 data is 14.61%. The high value of standard deviation for water may be explained by the wide range of data used to validate the present correlation, which includes 46 data from three different references at various experiment conditions.

Four models to predict the effective thermal conductivity of CNTs are compared with the present model by using the data from Tables 1 and 3. The models are shown in Eqs. (7), (10), (11) and (12), and the results of statistical calculations applied to the four models in comparison with the present correlation are shown in Table 6. The statistical calculations were achieved for water, polyalphaolefin and ethylene glycol separately, and for the all data together. However, the model by Patel et al. [59], represented by Eq. (10), was applied only to the water-based fluid data because the model requires the liquid particle size as an input. To ensure accuracy, the comparison for this model was restricted to water data, using the water particle size specified by Patel et al. [59] as shown in Table 6.

Table 5. The comparison of the predicted data found from the present correlation with the other models using the experimental data from Table 1 and 3.

Based on Table 1 and Table 3	Base fluid	Mean deviation (%)	Average deviation (%)	Standard deviation (%)	Number of data
By using Eq. (7)	Water	7.40	−4.76	9.14	124
	Polyalphaolefin	16.57	−16.57	22.52	11
	Ethylene glycol	6.40	3.21	7.96	19
	All data	7.93	−4.62	10.64	154
By using Eq. (10)	Water	31.04	23.53	52.11	124
By using Eq. (11)	Water	52.45	50.54	66.34	124
	Polyalphaolefin	62.88	59.23	111.35	11
	Ethylene glycol	104.60	104.60	159.95	19
	All data	59.63	57.83	87.60	154
By using Eq. (12)	Water	13.92	7.63	27.72	124
	Polyalphaolefin	18.07	−17.30	24.62	11
	Ethylene glycol	4.05	2.39	4.50	19
	All data	13.00	5.20	25.82	154
By using the present correlation, Eq. (2)	Water	8.53	−0.16	11.58	124
	Polyalphaolefin	12.62	−10.01	18.04	11
	Ethylene glycol	14.26	12.59	18.49	19
	All data	9.53	0.70	13.23	154

The results of standard deviation shown in Table 6, exhibit the minimum standard deviation for 154 data recorded for Eq. (7), and increased standard deviation for Eqs. (2), (12) and (11). However, a closer examination of the results shows that Eq. (7) works as a function for the nanoparticles volume fraction, so the only parameter that may affect the variation of the results is the volume fraction of nanoparticles. Accordingly, Eq. (7) produced similar results with temperature variation at a fixed CNT volume fraction. However, temperature has a significant effect on the effective thermal conductivity of the nanofluid, and similar results lead to a negligible reduction in the standard deviation. To further evaluate the four models, including Eq. (10), a detailed examination of the standard deviation for the water data was performed. The minimum standard deviation was obtained for the 124 water data points, which exhibited behaviour similar to that of the overall dataset and led to the same interpretation.

Equation (12) was generated based on experimental data for various nanoparticle types. Consequently, the model is not specific to CNTs. However, some data used to form the model were from experimental studies for CNTs, with the number of CNTs data lower than used in the present correlation. In addition, the present model considers the effect of CNTs length, which is an important parameter to be taken into account in the present correlation. According to the previous explanations, Eq. (12) can give accurate results with some limitations in comparison to the present correlation. Eq. (10) has limitations in the high temperatures of nanofluids, and Eq. (11), which was developed based on specific experimental data. Thus, these models show excellent results when applied to data within their specific calibration ranges. However, when evaluated against the wider range of data used in our study, they exhibit a higher standard deviation.

Another comparison was performed between the four models and the present correlation using specific experimental data in order to evaluate the mean, average and standard deviation for selected studies. The comparison presented in Fig. 2(a) is based on the experimental data of Wen and Ding [44]. As shown in Fig. 2(a), the minimum values of the mean, average and standard deviation were obtained using the present correlation. However, the applied data were part of the basic dataset used to develop the correlation. Figure 2(b) presents another comparison using the data of Jiang et al. [56], where the minimum values of the mean, average and standard deviation were obtained using Eq. (7), followed by the present correlation. It is important to note that the data used in Fig. 2(b) were obtained at a constant nanoparticle volume fraction and different temperatures.

The present correlation was applied to predict some properties of the CNTs/base fluid using CNTs with a thermal conductivity of 2000 W/(m·K) and density of 1900 kg/m³. The effective thermal conductivity versus temperature in the range of 293 K to 342 K and volume fraction in the range of 0.001 to 0.009 is shown in Fig. 3(a). The curve exhibits that effective thermal conductivity improved with the increasing CNTs volume fraction and temperature. The variation in the effective thermal conductivity with dynamic viscosity at CNTs volume fraction ranging from 0.001 to 0.009 and temperature ranging from 293 K to 342 K is shown in Fig. 3(b). The curve illustrates the decrease in the effective thermal conductivity with the increase in the dynamic viscosity, and enhancement in the effective thermal conductivity with the rising CNTs volume fraction. The dynamic viscosity affects the effective thermal conductivity of the nanofluid, and this relation is more pronounced at low dynamic viscosities. This behaviour agrees with the findings of Hassani et al. [50]. From the above explanation, it can be concluded that temperature affects the dynamic viscosity and consequently influences the effective thermal conductivity.

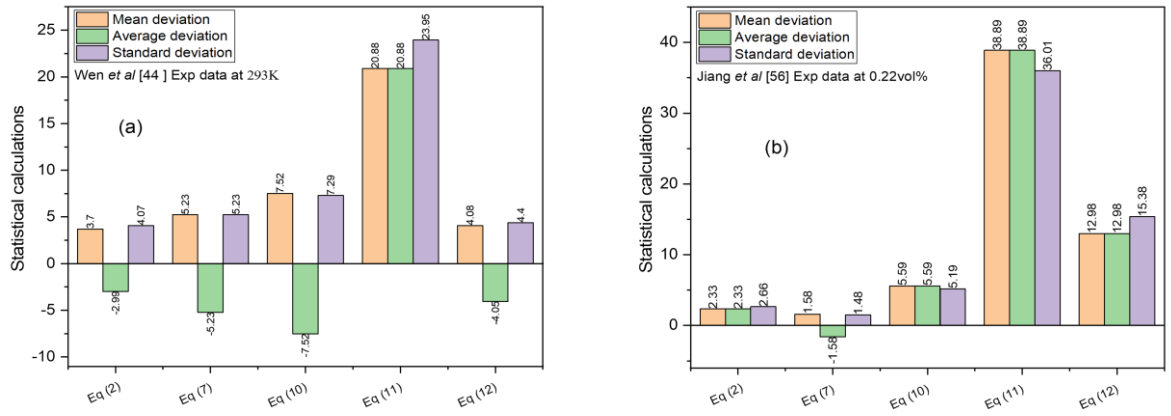

Fig. 2. Validation of the present correlation by comparison with other models for predicting the effective thermal conductivity using the experimental data of (a) Wen and Ding [44], (b) Jiang et al. [56].

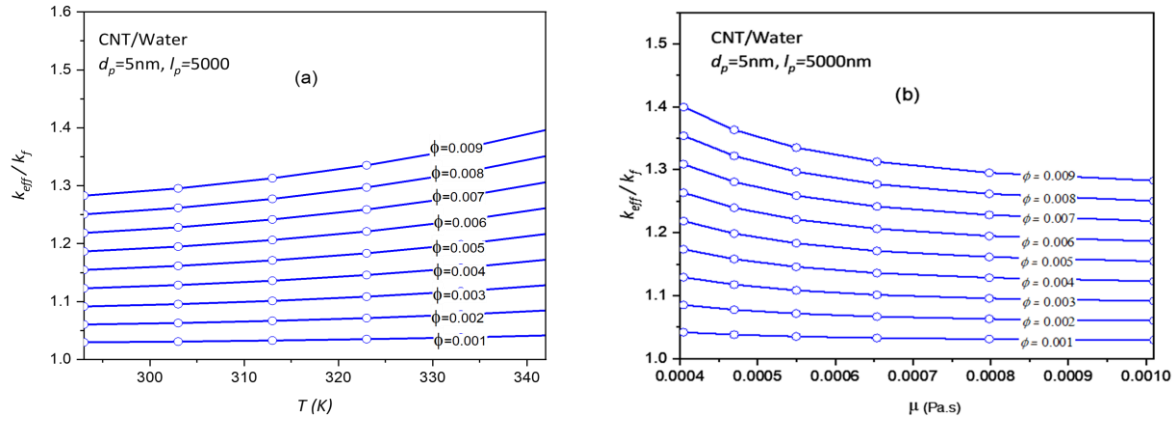

Fig. 3. Normalised thermal conductivity for CNTs/water found from the present correlation versus (a) temperature, (b) dynamic viscosity.

The effect of CNTs diameters on the effective thermal conductivity of the nanofluid is shown in Fig. 4(a), which exhibits an increase in the effective thermal conductivity of the nanofluid with the reduction in the CNTs diameter ranging from 1 nm to 100 nm, for CNTs volume fraction ranging from 0.3 to 1 % vol. at 298 K. Figure 4(b) shows the effect of CNTs length on the effective thermal conductivity of nanofluid, which increases with the increasing CNTs length ranging from 150 nm to 1000 nm, for CNTs volume fraction ranging from 0.3 to 1 % vol. at 298 K.

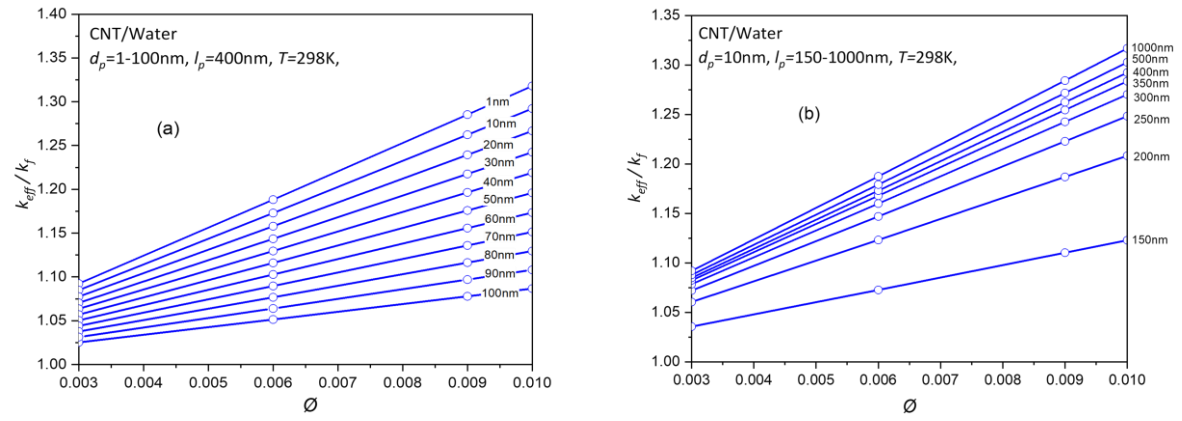

Fig. 4. Normalised thermal conductivity for CNTs/water found from the present correlation versus CNTs volume fraction at different (a) CNTs diameters, (b) CNTs lengths.

The effect of CNTs diameter on the effective thermal conductivity of CNTs/ethylene glycol is presented in Fig. 5(a). The effective thermal conductivity improved with the decreasing diameters of CNTs. The range of the used CNTs diameters is 1−40 nm, for CNTs volume fraction ranging from 0.3−1 % vol. at 298 K. Figure 5(b) indicates the effect of CNTs length on the effective thermal conductivity of CNTs/ethylene glycol. The curves exhibit an increase in the effective thermal conductivity

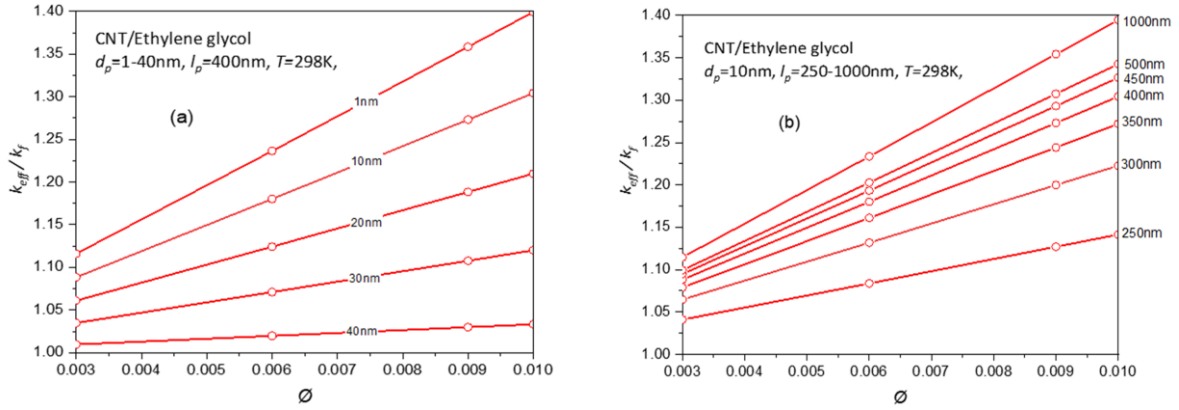

Fig. 5. Normalised thermal conductivity for CNTs/ethylene glycol found from the present correlation versus CNTs volume fraction at different (a) CNTs diameters, (b) CNTs lengths.

of the nanofluid with the increasing CNTs length ranging from 250 nm to 1000 nm, and CNTs volume fraction ranging between 0.3−1 % vol. at 298 K.

From Fig. 5(b) and Fig. 4(b), it can be noticed that the effective thermal conductivity is enhanced with the increasing CNTs length, and the amount of increase is reduced gradually with the increasing CNTs length over a specific value. In other words, the maximum improvement in the effective thermal conductivity was recorded at CNTs length from 250 nm to 300 nm, and decreased with the further increasing CNTs length, the minimum value found for 500 nm to 1000 nm. This behaviour can be interpreted by ballistic and ballistic-diffusive transport. The ballistic thermal transport takes place in CNTs of small length. The ballistic thermal transport produces a thermal resistance because of scattering of the phonon at the boundary, which improves the thermal conductivity. The ballistic-diffusive transport enhances with the increasing CNTs length, which occurs together with ballistic thermal transport and results in phonon scattering with both other phonons and the boundaries. Accordingly, the thermal resistance is generated because of the phonon-phonon scattering and phonon-boundary scattering, and whenever the CNTs length is increased, the phonon-boundary scattering is decreased. This interpretation agrees with the results of Cao and Qu [60], who determined that the length of zigzag single walled (SW) CNTs dominated by phonon-boundary scattering is ≤ 200 nm, and for armchair SW CNTs is ≤ 300 nm. Another interpretation related to the thermal boundary resistance, which controls the heat transfer at the interface between the base fluid and CNTs. Therefore, heat transfer improves when the thermal boundary resistance is small, and is reduced when it is high. Furthermore, since the effective thermal conductivity is a function of the CNT aspect ratio, as explained by Duong et al. [61], it improves with the increasing CNT length up to a point. The improvement of the effective thermal conductivity gets almost constant with the increasing CNTs length over a specific range due to the increase in the thermal boundary resistance that blocks the heat transfer. Duong et al. [61] determined the improvement in the effective thermal conductivity of SW CNTs/base fluid with an aspect ratio of SW CNTs reaching 80, and recorded almost a constant behaviour for the effective thermal conductivity for the SW CNTs aspect ratio greater than 80.

The comparison between the effective thermal conductivity of water and ethylene glycol at various volume fractions of CNTs, and at a fixed diameter and length, at 298 K, is shown in Fig. 6(a). The results indicate a higher effective thermal conductivity for CNTs/ethylene glycol than for CNTs/ water. This behaviour has been recorded in the experimental work presented by Harish et al [39], and compared with this work using the present correlation as shown in Fig. 6(b). A good agreement between the experimental and calculated data is found, which supports the validity of the present correlation.

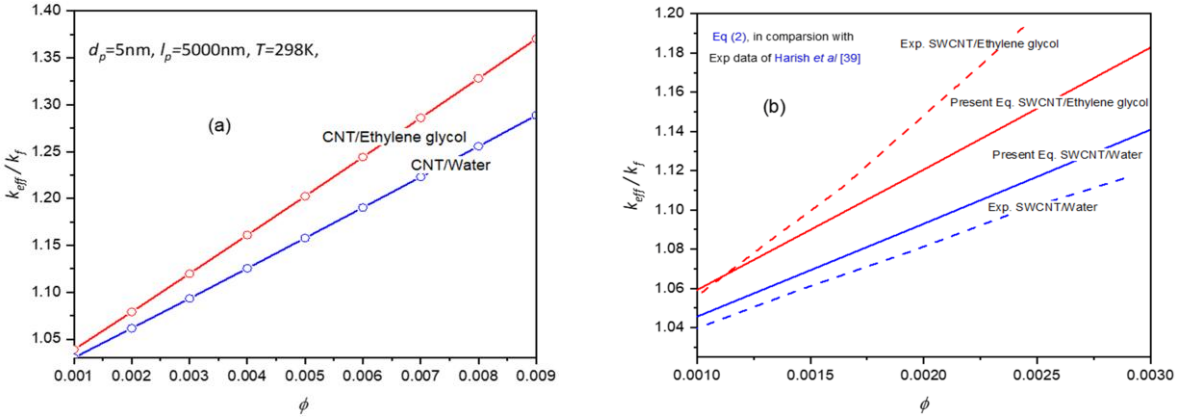

Fig. 6. Effective thermal conductivity versus CNTs volume fraction: (a) comparison between CNTs/ethylene glycol and CNTs/water (b) comparison between CNTs/ethylene glycol and CNTs/water with experimental work of Harish et al [39].

Research in this field remains active, with numerous recent studies providing experimental and theoretical insights into the effect of CNTs on the effective thermal conductivity of nanofluids. The models have been presented in these studies based on their specific empirical data, which reflect the conditions of their experiment.

To develop robust correlations for predicting the effective thermo-physical properties of nanofluids, periodic updates based on accumulating datasets are essential [62−64].

4. Limitations and future work

Although the present correlation was validated using a wide dataset of CNT nanofluids, it does not explicitly include the effects of particle aggregation and fluid stability, which can influence thermal conductivity through interfacial resistance and micro convection. Future work will incorporate these parameters and expand the database toward hybrid nanofluids and higher temperature ranges

5. Conclusions

A comprehensive correlation was developed to predict the effective thermal conductivity of CNT-based nanofluids by incorporating the combined effects of nanoparticle geometry (length and diameter), thermophysical properties of both the base fluid and CNTs, and operating temperature. The model was constructed through dimensional analysis and calibrated using 102 experimental data points from multiple literature sources, then validated on 52 independent datasets.

The correlation exhibited excellent agreement with experimental results, with low mean absolute percentage error and standard deviation, confirming its robustness and applicability for engineering analysis.

Comparative evaluation against several established models revealed that conventional correlations primarily depend on nanoparticle volume fraction and base-fluid conductivity while neglecting geometric characteristics. In contrast, the present model explicitly accounts for CNT length and diameter, demonstrating superior predictive accuracy and closer alignment with experimental data across a broad range of temperatures and concentrations.

The sensitivity analysis emphasised that the CNT aspect ratio (l/d), concentration and base-fluid viscosity are dominant factors influencing the effective thermal conductivity. These insights advance the understanding of nanoscale heat transport mechanisms and provide practical guidelines for the design and optimisation of thermal systems employing CNT nanofluids.

Although the proposed correlation performs effectively within its calibration range, future extensions should include nanoparticle aggregation and stability effects to enhance its applicability to hybrid nanofluids and high-temperature operations.

Overall, the developed correlation offers a reliable and physically consistent framework for predicting CNT nanofluid conductivity and represents a meaningful contribution toward accurate modelling of advanced nanofluid-based energy systems.

References

[1] Okonkwo, E.C., Wole-Osho, I., Almanassra, I.W., Abdullatif, Y.M., & Al-Ansari, T. (2021). An updated review of nanofluids in various heat transfer devices. *Journal of Thermal Analysis and Calorimetry*, 145(6), 2817–2872. doi: 10.1007/s10973-020-09760-2

[2] Choi, S.U.S., & Eastman, J.A. (1995). Enhancing thermal conductivity of fluids with nanoparticles *ASME International Engineering Congress & Exposition*, November 12−17, San Francisco, USA. Paper No. ANL/MSD/CP-84938; CONF-951135-29). https://www.osti.gov/biblio/196525 [accessed 17 Sept. 2025].

[3] Pordanjani, A.H., Aghakhani, S., Afrand, M., Mahmoudi, B., Mahian, O., & Wongwises, S. (2019). An updated review on application of nanofluids in heat exchangers for saving energy. *Energy Conversion and Management*, 198, 111886. doi: 10.1016/j.enconman.2019.111886

[4] Gupta, M., Singh, V., Kumar, R., & Said, Z. (2017). A review on thermophysical properties of nanofluids and heat transfer applications. *Renewable and Sustainable Energy Reviews*, 74, 638–670. doi: 10.1016/j.rser.2017.02.073

[5] Rashmi, W., Ismail, A.F., Sopyan, I., Jameel, A.T., Yusof, F., Khalid, M., & Mubarak, N.M. (2011). Stability and thermal conductivity enhancement of carbon nanotube nanofluid using gum arabic. *Journal of Experimental Nanoscience*, 6(6), 567–579.

[6] Zafarani-Moattar, M.T., & Majdan-Cegincara, R. (2013). Investigation on stability and rheological properties of nanofluid of ZnO nanoparticles dispersed in poly(ethylene glycol). *Fluid Phase Equilibria*, 354, 102–108. doi: 10.1016/j.fluid.2013.06.030

[7] Sabiha, M.A., Mostafizur, R.M., Saidur, R., & Mekhilef, S. (2016). Experimental investigation on thermo physical properties of single walled carbon nanotube nanofluids. *International Journal of Heat and Mass Transfer*, 93, 862–871. doi: 10.1016/j.ijheatmasstransfer.2015.10.071

[8] Sadri, R., Ahmadi, G., Togun, H., Dahari, M., Kazi, S.N., Sadeghinezhad, E., & Zubir, N. (2014). An experimental study on thermal conductivity and viscosity of nanofluids containing carbon nanotubes. *Nanoscale Research Letters*, 9(1), 151. doi: 10.1186/1556-276X-9-151

[9] Wen, D., & Ding, Y. (2004). Experimental investigation into convective heat transfer of nanofluids at the entrance region under laminar flow conditions. *International Journal of Heat and Mass Transfer*, 47(24), 5181–5188. doi: 10.1016/j.ijheatmasstransfer.2004.07.012

[10] Meisam, A., Ahmad, A., & Hamed, M. (2019). Experimental investigation of metal oxide nanofluids in a plate heat exchanger. *Journal of Thermophysics and Heat Transfer*, 33(4), 994–1005. doi: 10.2514/1.T5581

[11] Bianco, V., Chiacchio, F., Manca, O., & Nardini, S. (2009). Numerical investigation of nanofluids forced convection in circular tubes. *Applied Thermal Engineering*, 29(17–18), 3632–3642. doi: 10.1016/j.applthermaleng.2009.06.019

[12] Saeed, F.R., & Al-Dulaimi, M.A. (2021). Numerical investigation for convective heat transfer of nanofluid laminar flow inside a circular pipe by applying various models. *Archives of Thermodynamics*, 42(2), 71–95. doi: 10.24425/ather.2021.136948

[13] Phuoc, T.X., Massoudi, M., & Chen, R.H. (2011). Viscosity and thermal conductivity of nanofluids containing multi-walled carbon nanotubes stabilized by chitosan. *International Journal of Thermal Sciences*, 50(1), 12–18. doi: 10.1016/j.ijthermalsci.2010.09.008

[14] Vanaki, S.M., Ganesan, P., & Mohammed, H.A. (2016). Numerical study of convective heat transfer of nanofluids: A review. *Renewable and Sustainable Energy Reviews*, 54, 1212–1239. doi: 10.1016/j.rser.2015.10.042

[15] Maïga, S.E.B., Palm, S.J., Nguyen, C.T., Roy, G., & Galanis, N. (2005). Heat transfer enhancement by using nanofluids in forced convection flows. *International Journal of Heat and Fluid Flow*, 26(4), 530–546. doi: 10.1016/j.ijheatfluidflow.2005.02.004

[16] Masuda, H., Ebata, A., Teramae, K., & Hishinuma, N. (1993). Alteration of thermal conductivity and viscosity of liquid by dispersing ultra-fine particles (dispersion of γ-Al_2O_3, SiO_2 and TiO_2 ultra-fine particles). *Netsu Bussei*, 7(4), 227–233.

[17] Koo, J., & Kleinstreuer, C. (2005). Laminar nanofluid flow in microheat-sinks. *International Journal of Heat and Mass Transfer*, 48(13), 2652–2661. doi: 10.1016/j.ijheatmasstransfer.2005.01.029

[18] Das, S.K., Putra, N., Thiesen, P., & Roetzel, W. (2003). Temperature dependence of thermal conductivity enhancement for nanofluids. *Journal of Heat Transfer*, 125(4), 567–574. doi: 10.1115/1.1571080

[19] Chon, C.H., Kihm, K.D., Lee, S.P., & Choi, S.U.S. (2005). Empirical correlation finding the role of temperature and particle size for nanofluid (Al_2O_3) thermal conductivity enhancement. *Applied Physics Letters*, 87(15), 153107. doi: 10.1063/1.2093936

[20] Prasher, R., Bhattacharya, P., & Phelan, P.E. (2006). Brownian-motion-based convective-conductive model for the effective thermal conductivity of nanofluids. *Journal of Heat Transfer*, 128(6), 588–595. doi: 10.1115/1.2188509

[21] Sastry, N.N.V., Bhunia, A., Sundararajan, T., & Das, S.K. (2008). Predicting the effective thermal conductivity of carbon nanotube based nanofluids. *Nanotechnology*, 19(5), 055704. doi: 10.1088/0957-4484/19/05/055704

[22] Vajjha, R.S., & Das, D.K. (2009). Experimental determination of thermal conductivity of three nanofluids and development of new correlations. *International Journal of Heat and Mass Transfer*, 52(21–22), 4675–4682. doi: 10.1016/j.ijheatmasstransfer.2009.06.027

[23] Moghadassi, A., Hosseini, S.M., Henneke, D., & Elkamel, A. (2009). A model of nanofluids effective thermal conductivity based on dimensionless groups. *Journal of Thermal Analysis and Calorimetry*, 96(1), 81–84. doi: 10.1007/s10973-008-9843-z

[24] Hosseini, S.M., Moghadassi, A., & Henneke, D. (2011). Modelling of the effective thermal conductivity of carbon nanotube nanofluids based on dimensionless groups. *The Canadian Journal of Chemical Engineering*, 89(1), 183–186. doi: 10.1002/cjce.20389

[25] Emami-Meibodi, M., Vafaie-Sefti, M., Rashidi, A.M., Amrollahi, A., Tabasi, M., & Sid-Kalal, H. (2010). A model for thermal conductivity of nanofluids. *Materials Chemistry and Physics*, 123(2–3), 639–643. doi: 10.1016/j.matchemphys.2010.05.031

[26] Patel, H.E., Sundararajan, T., & Das, S.K. (2010). An experimental investigation into the thermal conductivity enhancement in oxide and metallic nanofluids. *Journal of Nanoparticle Research*, 12(3), 1015–1031. doi: 10.1007/s11051-009-9658-2

[27] Corcione, M. (2011). Empirical correlating equations for predicting the effective thermal conductivity and dynamic viscosity of nanofluids. *Energy Conversion and Management*, 52(1), 789–793. doi: 10.1016/j.enconman.2010.06.072

[28] Pak, B.C., & Cho, Y.I. (1998). Hydrodynamic and heat transfer study of dispersed fluids with submicron metallic oxide particles. *Experimental Heat Transfer*, 11(2), 151–170. doi: 10.1080/08916159808946559

[29] Lee, S., Choi, S.U.S., Li, S., & Eastman, J.A. (1999). Measuring thermal conductivity of fluids containing oxide nanoparticles. *Journal of Heat Transfer*, 121(2), 280–289. doi: 10.1115/1.2825978

[30] Eastman, J.A., Choi, S.U.S., Li, S., Yu, W., & Thompson, L.J. (2001). Anomalously increased effective thermal conductivities of ethylene glycol-based nanofluids containing copper nanoparticles. *Applied Physics Letters*, 78(6), 718–720. doi: 10.1063/1.1341218

[31] Yu, W., & Choi, S.U.S. (2003). The role of interfacial layers in the enhanced thermal conductivity of nanofluids. *Journal of Nanoparticle Research*, 5(1–2), 167–171. doi: 10.1023/A:1024438603801

[32] Chon, C.H., Kihm, K.D., Lee, S.P., & Choi, S.U.S. (2005). Empirical correlation finding the role of temperature and particle size for nanofluid (Al_2O_3) thermal conductivity enhancement. *Applied Physics Letters*, 87(15), 153107. doi: 10.1063/1.2093936

[33] Chon, C.H., & Kihm, K.D. (2005). Thermal conductivity enhancement of nanofluids by Brownian motion. *Journal of Heat Transfer*, 127(8), 810. doi: 10.1115/1.2033316

[34] Murshed, S.M.S., Leong, K.C., & Yang, C. (2008). Investigations of thermal conductivity and viscosity of nanofluids. *International Journal of Thermal Sciences*, 47(5), 560–568. doi: 10.1016/j.ijthermalsci.2007.05.004

[35] Mintsa, H.A., Roy, G., Nguyen, C.T., & Doucet, D. (2009). New temperature dependent thermal conductivity data for water-based nanofluids. *International Journal of Thermal Sciences*, 48(2), 363–371. doi: 10.1016/j.ijthermalsci.2008.03.009

[36] Duangthongsuk, W., & Wongwises, S. (2009). Measurement of temperature-dependent thermal conductivity and viscosity of TiO_2-water nanofluids. *Experimental Thermal and Fluid Science*, 33(4), 706–714. doi: 10.1016/j.expthermflusci.2009.01.005

[37] Azmi, W.H., Sharma, K.V., Mamat, R., Alias, A.B.S., & Misnon, I.I. (2012). Correlations for thermal conductivity and viscosity of water based nanofluids. *IOP Conference Series: Materials Science and Engineering*, 36(1), 012029. 5–7 December 2011, Kuantan, Pahang, Malaysia. doi: 10.1088/1757-899X/36/1/012029

[38] Hosseini, S.M., Safaei, M.R., Goodarzi, M., Alrashed, A.A.A.A., & Nguyen, T.K. (2017). New temperature, interfacial shell dependent dimensionless model for thermal conductivity of nanofluids. *International Journal of Heat and Mass Transfer*, 114, 207–210. doi: 10.1016/j.ijheatmasstransfer.2017.06.061

[39] Harish, S., Ishikawa, K., Einarsson, E., Aikawa, S., Inoue, T., Zhao, P., Watanabe, M., Chiashi, S., Shiomi, J., & Maruyama, S. (2012). Temperature dependent thermal conductivity increase of aqueous nanofluid with single walled carbon nanotube inclusion. *Materials Express*, 2(3), 213–223. doi: 10.1166/mex.2012.1074

[40] Choi, S.U.S., Zhang, Z.G., Yu, W., Lockwood, F.E., & Grulke, E.A. (2001). Anomalous thermal conductivity enhancement in nanotube suspensions. *Applied Physics Letters*, 7(14), 2252–2254. doi: 10.1063/1.1408272

[41] Lamas, B.C., Fonseca, A., Gonçalves, F.A.M M., Ferreira, A.G.M., Fonseca, I.M.A., Kanagaraj, S., Martins, N., & Oliveira, M.S.A. (2011). EG/CNTs nanofluids engineering and thermo-rheological characterization. *Journal of Nano Research*, 13, 69−74. doi: 10.4028/www.scientific.net/JNanoR.13.69

[42] Nanda, J., Maranville, C., Bollin, S.C., Sawall, D., Ohtani, H., Remillard, J.T., & Ginder, J.M. (2008). Thermal conductivity of single-wall carbon nanotube dispersions: Role of interfacial effects. *The Journal of Physical Chemistry C*, 112(3), 654–658. doi: 10.1021/jp711164h

[43] Xie, H., Lee, H., Youn, W., & Choi, M. (2003). Nanofluids containing multiwalled carbon nanotubes and their enhanced thermal conductivities. *Journal of Applied Physics*, 94(8), 4967–4971. doi: 10.1063/1.1613374

[44] Wen, D., & Ding, Y. (2004). Effective thermal conductivity of aqueous suspensions of carbon nanotubes (carbon nanotube nanofluids). *Journal of Thermophysics and Heat Transfer*, 18(4), 481–485. doi: 10.2514/1.9934

[45] Hwang, Y.J., Ahn, Y.C., Shin, H.S., Lee, C.G., Kim, G.T., Park, H.S., & Lee, J.K. (2006). Investigation on characteristics of thermal conductivity enhancement of nanofluids. C*urrent Applied Physics*, 6(6), 1068–1071. doi: 10.1016/j.cap.2005.07.021

[46] Walvekar, R., Faris, I.A., & Khalid, M. (2012). Thermal conductivity of carbon nanotube nanofluid—experimental and theoretical study. *Heat Transfer—Asian Research*, 41(2), 145–163. doi: 10.1002/htj.20405

[47] Almanassra, I.W., Manasrah, A.D., Al-Mubaiyedh, U.A., Al-Ansari, T., Malaibari, Z.O., & Atieh, M.A. (2020). An experimental study on stability and thermal conductivity of water/CNTs nanofluids using different surfactants: A comparison study. *Journal of Molecular Liquids*, 304, 111025. doi: 10.1016/j.molliq.2019.111025

[48] Vaschy, A. (1892). On the laws of similarity in physics. *Annales Télégraphiques*, 19, 25–28.

[49] Buckingham, E. (1914). On physically similar systems; illustrations of the use of dimensional equations. *Physical Review*, 4(4), 345–376.

[50] Hassani, S., Saidur, R., Mekhilef, S., & Hepbasli, A. (2015). A new correlation for predicting the thermal conductivity of nanofluids; using dimensional analysis. *International Journal of Heat and Mass Transfer*, 90, 121–130. doi: 10.1016/j.ijheatmasstransfer.2015.06.040

[51] Koo, J., & Kleinstreuer, C. (2004). A new thermal conductivity model for nanofluids. *Journal of Nanoparticle Research*, 6(6), 577–588. doi: 10.1007/s11051-004-3170-5

[52] Kumar, K.V., Preuss, K., Titirici, M.M., & Rodríguez-Reinoso, F. (2011). Molecular simulation of hydrogen physisorption and chemisorption in nanoporous carbon structures. *Adsorption Science and Technology*, 29(8), 799–817. doi: 10.1260/0263-6174.29.8.799

[53] Xu, X., Yang, W., Song, C., Liu, J., & Lin, L. (2003). Hydrogen separation by zeolite membranes. *ACS Division of Fuel Chemistry*, 48(1), 284–285.

[54] Harish, S., Ishikawa, K., Einarsson, E., Aikawa, S., Chiashi, S., Shiomi, J., & Maruyama, S. (2012). Enhanced thermal conductivity of ethylene glycol with single-walled carbon nanotube inclusions. *International Journal of Heat and Mass Transfer*, 55(13–14), 3885–3890. doi: 10.1016/j.ijheatmasstransfer.2012.03.001

[55] Halelfadl, S., Maré, T., & Estellé, P. (2014). Efficiency of carbon nanotubes water based nanofluids as coolants. *Experimental Thermal and Fluid Science*, 53, 104–110. doi: 10.1016/j.expthermflusci.2013.11.010

[56] Jiang, H., Zhang, Q., & Shi, L. (2015). Effective thermal conductivity of carbon nanotube-based nanofluid. *Journal of the Taiwan Institute of Chemical Engineers*, 55, 76–81. doi: 10.1016/j.jtice.2015.03.037

[57] Sadri, R., Ahmadi, G., Togun, H., Dahari, M., Kazi, S.N., Sadeghinezhad, E., & Zubir, N. (2014). An experimental study on thermal conductivity and viscosity of nanofluids containing carbon nanotubes. *Nanoscale Research Letters*, 9(1), 151. doi: 10.1186/1556-276X-9-151

[58] Hamilton, R.L., & Crosser, O.K. (1962). Thermal conductivity of heterogeneous two-component systems. *Industrial & Engineering Chemistry Fundamentals*, 1(3), 187–191. doi: 10.1021/i160003a005

[59] Patel, H.E., Anoop, K.B., Sundararajan, T., & Das, S.K. (2008). Model for thermal conductivity of CNT-nanofluids. *Bulletin of Materials Science*, 31(3), 387–390. doi: 10.1007/s12034-008-0060-y

[60] Cao, A., & Qu, J. (2012). Size dependent thermal conductivity of single-walled carbon nanotubes. *Journal of Applied Physics*, 112(1), 013503. doi: 10.1063/1.4730908

[61] Duong, H.M., Papavassiliou, D.V., Mullen, K.J., Wardle, B.L., & Maruyama, S. (2008). Calculated thermal properties of single-walled carbon nanotube suspensions. *The Journal of Physical Chemistry C*, 112(50), 19860–19865. doi: 10.1021/jp710021n

[62] Qin, J., Tao, Y., Liu, Q., Li, Z., Zhu, Z., & He, N. (2023). Experimental and theoretical studies of different parameters on the thermal conductivity of nanofluids. *Micromachines*, 14(5), 964. doi: 10.3390/mi14050964

[63] Mahdi, E.J., Hussein, H.F., Hassoon, I.A., & Jasim, A.A.-A. (2025). Analysis of solar panel surface thermal distribution using thermal imaging. *Journal of Renewable Energy and Environment*, 12(4), 74–80. doi: 10.30501/jree.2025.495645.2207

[64] Sarkar, S., Pal, P., & Ghosh, N.K. (2024). Enhancing the thermal conductivity and viscosity of ethylene glycol-based single-walled carbon nanotube (SWCNT) nanofluid: An investigation utilizing equilibrium molecular dynamics simulation. *Chemical Thermodynamics and Thermal Analysis*, 16, 100142. doi: 10.1016/j.ctta.2024.100142

[65] Hussein, H.F., Druga, L., Cojocaru, M., Dumitru, C., & Ghinea, A. (2018). Predicting and monitoring eutectic carbides proportion in cast austenitic Cr–Ni stainless steels. *U.P.B. Scientific Bulletin, Series B: Chemistry and Materials Science*, 80(4), 169–180.

[66] Hussein, H.F., Druga, L., Cojocaru, M., Dumitru, C., & Ghinea, A. (2020). The structural evolution of refractory steel spare parts during the successive carburizing. *U.P.B. Scientific Bulletin, Series B: Chemistry and Materials Science*, 82(1), 247–257.

[67] Batros, S.S., Saeed, F.R., & Hussein, H.F. (2025). Antibacterial activity and microstructure properties of copper oxide particles doped with cadmium prepared by chemical precipitation method. *Iranian Journal of Materials Science and Engineering*, 22(1), 107–117. doi: 10.22068/ijmse.3864

[68] Obaid, A.H., Mahdi, E.J., Hassoon, I.A., Hussein, F.H., Jasime, A.A.A-S., Jafar, A.N., & Abdulghani, A.S. (2024). Evaluation of degradation factor effect on solar panels performance after eight years of life operation. *Archives of Thermodynamics*, 45(3), 221–226. doi: 10.24425/ather.2024.151223

[69] Mahdi, E.J., Hussein, H.F., & Saeed, F.R. (2025). Thermal performance comparison of aluminum and iron alloys in heat exchangers for solar water-heating systems: Experimental study under Iraqi climate conditions. *Next Materials*, 8, 100935. doi: 10.1016/j.nxmate.2025.100935

[70] Hasoon, I.A., Inad, K.I., Mahdi, E.J., Salih, S.M. & Hussein, H.F. (2025). Design and performance evaluation of an off-grid photovoltaic system for metallurgical laboratories. *JOM (Journal of The Minerals, Metals & Materials Society)*, 77, 10158−10164. doi: 10.1007/s11837-025-07867-1

[71] Ahmed, S.B., Al-Naemi, A.N.A., Kamar, F.H., Hussein, H.F., & Nawar, M.S. (2024). Adsorption of phenol from aqueous solution using graphene nano-particles. *The 4th International Conference on Sustainable Engineering Techniques*, 5−6 October, Baghdad, Iraq. *AIP Conference Proceedings*, 3105(1), 070003. doi: 10.1063/5.0212296